Indentation cracking in silicate glasses is directed by shear flow, not by densification

Etienne Barthel, Vincent Keryvin, Gustavo Rosales-Sosa, Guillaume Kermouche

Indentation cracking in silicate glasses is directed by shear flow, not by densification

Etienne Barthel[a], Vincent Keryvin[b], Gustavo Rosales-Sosa[c], Guillaume Kermouche[d]

[a] *Soft Matter Sciences and Engineering, ESPCI Paris, PSL University, CNRS, Sorbonne University, 75005 Paris, France.*
[b] *Univ. Bretagne Sud, UMR CNRS 6027, IRDL, F-56321 Lorient, France*
[c] *Nippon Electric Glass, 7-1, Seiran 2-Chome, Otsu, 520-8639, Shiga, Japan*
[d] *Mines Saint-Etienne, Univ Lyon, CNRS, UMR 5307 LGF, Centre SMS, F - 42023 Saint-Etienne France*

Abstract

Over the past decades, constitutive relations have been developed to compute the mechanical response of silicate glasses at the continuum length scale. They are now reliable enough that we can calculate indentation induced stress and strain fields and examine the impact of material parameters on indentation response, and especially hardness, pile-up and stress fields. In contrast to a presently widespread assumption in the literature, we show that (shear) flow stress is the primary determinant of these properties, and that densification plays a secondary role in the indentation response of all the silicate glasses. This result applies even for large values of the densification at saturation because of the high ratio between effective volumetric yield stress (*i.e.* yield pressure) and flow stress.

It is well-known that, depending upon composition, silicate glasses exhibit very different sensitivities to indentation cracking, although all other standard mechanical properties remain quite similar. We point out that material damage incurred through plastic shear flow, and especially shear flow instability and localization may well control crack initiation, which would resolve the paradox. Shear flow instability and damage has not been quantitatively investigated in detail in silicate glasses as yet, neither experimentally nor theoretically. However, we believe it is key to an in depth understanding of cracking resistance in silicate glasses.

Keywords:
Silicate glasses, Plasticity, Indentation cracking, densification, Constitutive relation

1. Introduction

Because it is the archetypal damage process, indentation cracking of silicate glasses has been extensively studied over the past century [1, 2, 3]. It has been

clearly established that the final crack pattern and the cracking sequence during a full indentation cycle strongly depend not only upon maximum load but also on the composition of the glass [4, 5, 6] and the sharpness of the indenter [7, 8]. However, the cracking process is still largely ill-understood [9, 10]. Better insight would hopefully pave the way to the formulation of more resistant glasses.

In silicate glasses as in other materials, plastic deformation is central to the stress field which develops during indentation. However, in contrast to metallic materials or polymers, it has been demonstrated that plastic deformation in silicate glasses sometimes involves permanent volumetric strain, ie densification [11]. The phenomenon is particularly notable in amorphous silica. Because densification is absent in the more conventional metal plasticity, it has attracted considerable interest in the glass community. It turns out that amorphous silica, which exhibits the highest level of densification among silicate glasses, also features a specific crack pattern upon indentation, with ring and cone cracks [2]. As a result, the connections between densification and crack patterns have been investigated using various tools, among which the most prominent is the stress distribution model proposed by Yoffe [2, 4].

In Yoffe's model [12], an approximate form for the contribution of the stress field due to plastic strain is proposed (the so-called blister field) and the intensity of this blister field has been diversly evaluated. Various quantities have been used from hardness to modulus ratio, proportionally corrected by densification [2] to elaborate measurements of volumes below and above the surface after and before annealing [4]. Some insight has been gained by this method, but two shortcomings can be identified: 1) the determination of the amplitude of the blister field (representing the role of plastic deformation) is not unequivocal, and 2) the degree of approximation of the model is unknown.

As a result, the question of the relation between glass structure and indentation cracking is still a largely unsolved question, despite huge technological implications. Alternative methods to understand the stress field developing during indentation in silicate glasses and the response of the material to this stress field would be highly useful. Here we present numerical results based on a recently developed constitutive relation [13] for silicate glasses. It has been validated for amorphous silica under a few different loading configurations, and provides reasonable agreement with all the measured mechanical properties of amorphous silica, including densification. While still an approximation, we believe that it provides an acceptable description of plastic deformation during indentation of silicate glasses. We use it to evaluate the impact of each of the relevant material parameters identified in the constitutive model. Three characteristic phenomena registered in the indentation of silicate glasses will be considered: 1) macroscopic response, *i.e.* hardness; 2) pile-up formation and 3) stress and strain fields, which we will discuss in relation to crack formation in silicate glasses. Our conclusion is that the role of densification has been largely overemphasized in the past decades. We point out that beyond densification at saturation, a key parameter is the ratio of the effective yield pressure to flow stress, which is always too large for densification to play a significant role in the indentation response of silicate glasses. As a result, shear flow dominates over

densification even in amorphous silica, and the flow stress – or more precisely the ratio of the flow stress to Young's modulus – is the first order parameter.

Within this wider point of view, the diversity of cracking behaviour in silicate glasses cannot be accounted for. This shortcoming strongly suggests that local damage – which may in many cases be induced by the localization of shear flow – must be taken into account to obtain a full picture of cracking in silicate glasses. This conjecture opens up new perspectives for the understanding of cracking resistance in silicate glasses.

2. Model

2.1. Constitutive relation

To model the response of silicate glasses at the continuum lengthscale, we use a constitutive model which has been tested over the last decade [13]. In brief, elasticity is assumed linear isotropic and is characterized by Young's modulus and Poisson's ratio. Plastic strain is triggered when a criterion depending elliptically upon hydrostatic pressure and shear stress is met (Fig. 1).

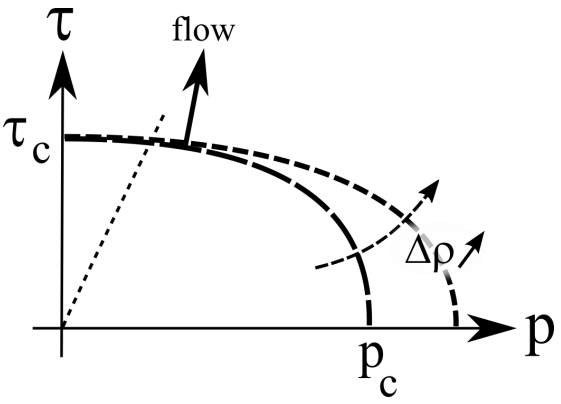

Figure 1: Elliptic yield criterion for the plastic response of silicate glasses [13] characterized by flow stress τ_c and yield pressure p_c. The yield pressure itself increases with densification $\Delta\rho$ while the flow stress is assumed to be independent of plastic strains. The straight dashed line represents uniaxial compression.

In Fig. 1, $\tau = \sqrt{\frac{3}{2}\,\mathrm{tr}\,(\underset{\sim}{s}\cdot\underset{\sim}{s})}$ where $\underset{\sim}{s}$ is the deviatoric part of the Cauchy stress tensor and tr is the trace operator.

This criterion is characterized by: 1) the flow stress τ_c, ie the uniaxial (Mises) stress at which plastic deformation occurs (here we have adopted the notation τ_c to emphasize the nature of this deformation, which is plastic shear flow) and 2) the volumetric yield stress or yield pressure p_c, ie the pressure at which densification occurs under pure hydrostatic compression. Based on high pressure hydrostatic experiments, p_c itself is known to depend upon the current density of the material until a saturation density is reached: this hardening is built into

the model [13, 14]. We also assume that shear flow does not result in hardening or softening. For silica, the validity of this assumption has been demonstrated experimentally [15]. For other glasses, this is more of an approximation and its possible shortcomings will be pointed out in the discussion. The partition of plastic strain between densification and shear flow is set by a condition of normality of flow relative to the yield surface (associated plasticity). Given the horizontal slope near the pure shear axis, plastic strain will be predominantly shear flow in this region of loading state. Conversely, given the vertical slope near the pure pressure axis, plastic strain will be predominantly densification in this region. If the loading contains both shear stress and pressure in a significant measure, densification and shear flow will concur to plastic strain in a ratio which is set by the direction of the normal to the yield surface. In brief, in this simplified model, the main parameters for the plastic part of the constitutive relation are the flow stress, the yield pressure, a hardening slope *for the yield pressure* and the saturation density. From the original density ρ and this saturation density ρ_{sat} we can derive the densification at saturation $\Delta\rho_{sat} = \rho_{sat}/\rho - 1$ which is directly related to the free volume in the pristine material ϕ by the relation $\phi = \Delta\rho_{sat}/(1 + \Delta\rho_{sat})$.

More quantitatively, for a reference material approximating amorphous silica, we will use a flow stress τ_c=7.0 GPa, a yield pressure p_c=9.0 GPa and a densification at saturation $\Delta\rho_{sat} = 0.20$. Maximum densification is reached at a pressure of 20 GPa. The parameter values typical for other glasses will be defined in comparison to this reference material.

Two standard indenter geometries have been considered, a Vickers and its axisymmetric (conical) analog. Due to self-similarity, the dimension of the system is irrelevant. However, numerical accuracy will depend upon both the ratio of the mesh size to the contact radius under load and the ratio of the contact radius to the system size. The mesh is refined in the indentation region. Typically we use a contact radius equal to 45 times the element size, a lateral system size equal to 15 times the contact radius, and a vertical system size 1.5 times larger than the lateral size. The calculations are performed with Abaqus 2016 using about 4000 CAX4 elements in the axisymmetric model and about 130000 C3D8 elements in the Vickers model. A UMAT file containing an implementation of the Kermouche constitutive relation [13, 16] is provided as supplementary material.

3. Results

3.1. Macroscopic response - hardness

Hardness is a complicated material property which encapsulates in one figure the macroscopic, integrated response of an elastoplastic material to sharp contact. The simplest evaluation of hardness is obtained with a standard microindenter, where the applied force is simply divided by the area of the imprint after unloading. In instrumented indentation [17], the force applied to the indenter is measured continuously as a function of penetration. In this case, with

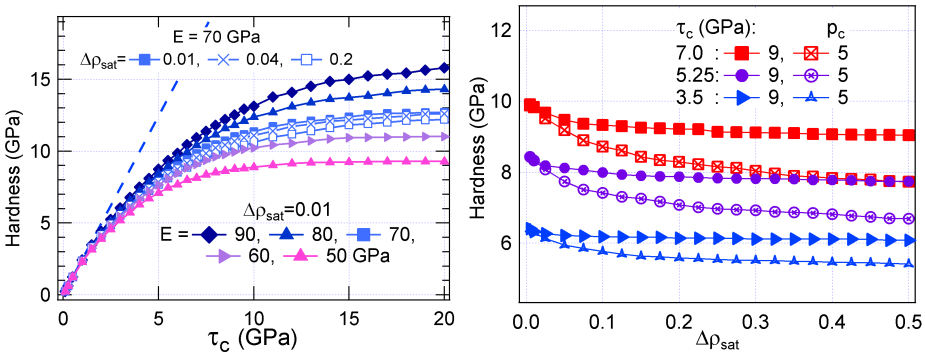

Figure 2: Calculated hardness (*i.e.* mean contact pressure) for a cone equivalent to a Vickers indenter. Left: hardness as a function of flow stress for a yield pressure $p_c = 9$ GPa and negligible densification at saturation ($\Delta\rho_{sat} = 0.01$). The calculations were repeated for a few values of Young's modulus spanning the 50 to 90 GPa range. Poisson's ratio is 0.2. For a Young's modulus of 70 GPa, we also calculated hardness for larger values of $\Delta\rho_{sat}$: there is only a slight decrease of hardness when densification at saturation increases from 0.01 to 0.20. Right: hardness as a function of densification at saturation for $\tau_c = 3.5$, 5.25 and 7.0 GPa and for two different values of yield pressure. For all three values of flow stress, hardness decreases moderately with densification at saturation for $p_c = 9$ GPa, and much more markedly for $p_c = 5$ GPa.

adequate data analysis, one can obtain an evaluation of hardness more closely related to the definition, *i.e.* contact force normalized by contact area, or mean contact pressure under load [17]. Due to the self-similarity of the problem, it is a constant. In our numerical calculations, a constant mean contact pressure is indeed found, and it is this value which is taken for hardness.

Calculated hardness as a function of flow stress is shown in Fig. 2 (left) for a yield pressure p_c=9 GPa, a negligible densification at saturation $\Delta\rho_{sat} = 0.01$ and different Young's modulus. Poisson's ratio is always $\nu = 0.2$ except when mentioned otherwise. Hardness initialy grows linearly with flow stress then slackens for flow stresses larger than *ca.* 3 GPa and reaches a plateau at large τ_c. This plateau marks a purely elastic response and is here particularly visible for the lower values of Young's modulus. A first idea of the impact of densification at saturation on hardness can be garnered by the results for $\Delta\rho_{sat} = 0.04$, with a very moderate decrease of hardness (here Young's modulus is $E = 70$ GPa, our reference value). Even increasing densification at saturation to 0.20, which is the largest conceivable value for silicate glasses, and found only in amorphous silica, we find only a minute reduction of the calculated hardness, less than 5 %. What ostensibly appears is that a reduction of the Young's modulus by 15% has more effect on hardness than a 20 times reduction of densification at saturation !

To gain insight into this potentially surprising result, calculated hardness as a function of densification at saturation is shown in Fig. 2 (right) for a Young's modulus $E = 70$ GPa, a yield pressure p_c=9 GPa and three different values of the flow stress 7, 5.25 and 3.5 GPa. Hardness decreases with densification

at saturation in all cases with a *ca* 10% decrease over the $\Delta\rho_{sat} = 0$ to 0.5 range for τ_c=7 GPa. The decrease is even smaller for lower values of τ_c. These evolutions bring to light a competition between volumetric deformation and shear flow. Significant impact on hardness is found only when the yield pressure is stepped down from 9 to 5 GPa, with a near 20% reduction in hardness at 0.20 densification at saturation for τ_c=7 GPa. Clearly, the role of densification in indentation depends not only on the densification at saturation, but also on the balance between flow stress and yield pressure. With a high yield pressure, the balance will lean in favour of flow deformation.

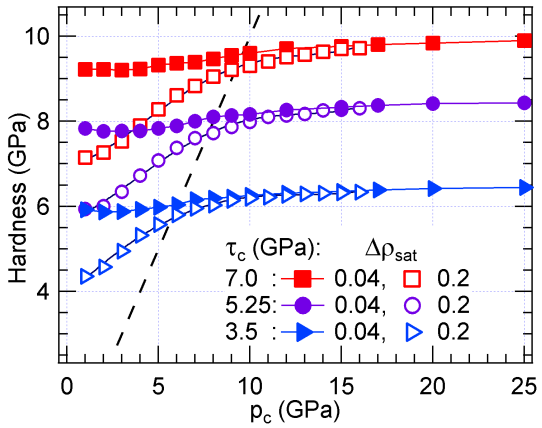

Figure 3: Calculated hardness for a Vickers equivalent cone as a function of yield pressure for τ_c = 3.5, 5.25 and 7.0 GPa, and small (0.04) or large (0.20) densification at saturation. Even with sizeable densification at saturation, hardness remains insensitive to densification when the yield pressure exceeds a threshold, which, in the parameter range relevant here, is roughy equal to the hardness (dashed line).

To better appreciate this effect, hardness calculated as a function of yield pressure p_c is shown in Fig. 3 for three values of the flow stress 3.5, 5.25 and 7.0 GPa and two values of the densification at saturation 0.04 and 0.2. We indeed find that the effect of densification at saturation is observed at lower values of the yield pressure, and that the threshold decreases slowly with flow stress. However the effect is mostly noticeable for a $\Delta\rho_{sat} = 0.2$ densification at saturation but almost vanishes when the densification at saturation drops to 0.04.

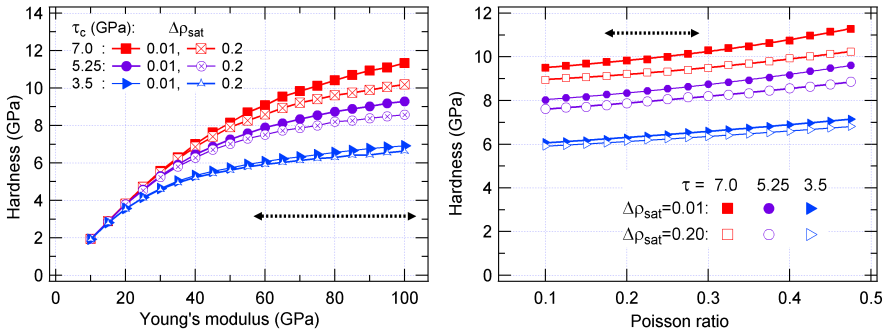

Figure 4: Calculated hardness for a Vickers equivalent cone. Left: hardness as a function of Young's modulus for yield pressure p_c =9 GPa, flow stress τ_c = 3.5, 5.25 and 7.0 GPa, and small (0.01) or large (0.20) densification at saturation. Poisson's ratio is ν = 0.2. Hardness increases with Young's modulus. Right: hardness also increases but very moderately with Poisson's ratio. The dashed segments mark the ranges of parameters relevant for most silicate glasses.

Finally, for completeness, we investigate the impact of *elastic* material properties on indentation response. Calculated hardness is shown in Fig. 4 as a function of Young's modulus (left - ν =0.2) and Poisson's ratio (right - E =70 GPa), for a yield pressure 9 GPa, three values of the flow stress 3.5, 5.25 and 7.0 GPa and two values (high - 0.20 and low - 0.01) of densification at saturation. As expected from the previous graphs, hardness increases with Young's modulus, and this increase is larger for larger flow stress. Hardness increases by as much as 30% over the modulus range 50-90 GPa for τ_c=7 GPa, and by half this value for τ_c=3.5 GPa.

Hardness also increases moderately with Poisson's ratio. More specifically, focusing on the range relevant for silicate glasses, we find that hardness increases by about 10% over the range of Poisson's ratio 0.15-0.3. The effects of flow stress and densification at saturation on the *evolution* of hardness with Poisson's ratio, however, are weak.

In brief, as a rule of thumb, densification will have a noticeable impact on hardness if: 1) the densification at saturation is large and 2) the yield pressure is moderate, compared to the flow stress. Note that when talking loosely about yield pressure here, we implicitly refer to an effective value which involves the effect of volumetric strain hardening. One must therefore keep in mind that this effective yield pressure is typically larger than p_c. Focusing on amorphous silica, for which the constitutive relation used here is best calibrated, we conclude that densification does affect hardness, but only moderately, certainly not as much as is sometimes implied given the large densification at saturation (ca 0.20). The primary reason is that the *yield pressure* is comparable (9 GPa) to the *flow stress* (7 GPa) and that due to volumeric hardening the effective yield pressure is somewhat larger, thus effectively restricting material compaction during indentation. We conclude that plastic deformation during indentation with Vickers type indenters, even in amorphous silica, is dominated by shear

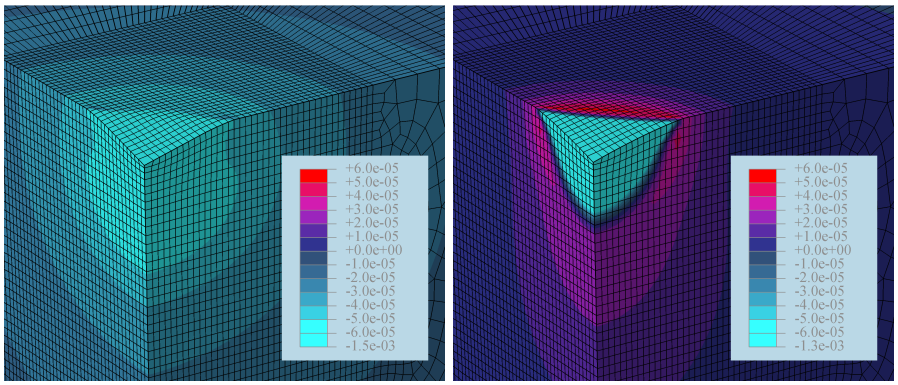

Figure 5: Vickers indentation: distribution of vertical displacement u_z ($\tau_c = 3.5$ GPa, $p_c = 7$ GPa, $\Delta\rho_{sat} = 0.04$) near the end of unloading (left - $F = 0.25F_{max}$) and after complete unloading (right - $F = 0$). The maximum penetration was 2.0 10^{-3}. Upward displacements are colored in purple-red hues while downward displacements are in turquoise. The plastically deformed core is pushed back by the elastically stressed half space resulting in the appearance of pile-up at the very end of the unloading process.

flow, and that hardness depends first and foremost upon the flow stress (Fig. 2).

Based on the present results, it is clear that similar conclusions will apply to a material with low densification at saturation such as the so-called normal glasses. To approximate soda-lime silica glass, from literature data, and within the present model, we reduce the flow stress to 3.5 GPa, the yield pressure to 7 GPa and densification at saturation to 0.04 [18, 19]. We also set hardening such that density saturates at 16 GPa, a minor variation compared to the cases previously calculated. Here again, the conclusion is that hardness is dominated by flow stress (not shown).

3.2. Indentation kinematics and the formation of pile-ups

Pile-up has been found on indent edges in some glasses [20, 21]. To better understand the kinematics of formation of these pile-ups, a Vickers indentation has been calculated for a soda-lime glass analog, for a maximum penetration of 2 μm. The distribution of vertical displacement is shown in Fig. 5 at 3/4 of unloading (left) and after full unloading (right). During loading and most of unloading, all vertical displacements point downwards (turquoise blue). In contrast, net upward vertical displacements (shown in purple-red hues) only appear at the very end of unloading. They develop all around the indent, including at the surface, along the faces, where they are easily measurable by AFM. For the amorphous silica analog (see above), our calculations show that pile-up does form as well, but with considerably reduced amplitude. This process, whereby the pile-up appears only at the very end of unloading, is very different from a pile-up which would form through extensive shear flow alongside the indenter faces during loading. It shows that for silicate glasses pile-ups form when the plasticaly deformed core, under the indenter, is pushed back by the elastically stressed half space as the load is removed.

3.3. Stress field

As already mentioned, understanding the stress field which develops during indentation is presently one of the major goals of glass mechanics research, with a view to hopefully improving material formulation. Experiments and models such as Yoffe's are primarily developed to improve our understanding of the stress field and how it leads to cracking. Because stress fields are 2nd rank tensors, and strongly depend not only on material parameters but also on loading history, a full account of our numerical results would be exceedingly tedious and will not be attempted here. We only wish to demonstrate that the stress fields derived from the present constitutive relation are at least as consistent with the crack patterns found in various types of silicate glasses as Yoffe's model.

For our soda-lime glass analog, we have calculated the stress field during Vickers indentation. For such a glass, a crack type of prominent interest is the median-radial system, which typically appears during unloading [2]. With the z direction along the indentation axis, we monitor the σ_{yy} stresses, which are normal to the diagonal planes of the Vickers indent. The σ_{yy} stresses after full unloading are plotted on Fig. 6 left. Tensile stresses appear, which are maximum at the surface in the vicinity of the indenter edges; in fact, we observe in our calculations that tensile stresses are already present upon loading, but intensify markedly upon unloading. These characteristics match the appearance of radial cracks outside the indent along the indenter edge directions. In normal glasses, they indeed usually appear in the early stages of unloading [2].

We now turn to the σ_{zz} stress component. We find that this component is *compressive* all along the loading and unloading phases, *except* at the very end of unloading when it abruptly turns tensile (Fig. 6 right). In fact, stress inversion and surface uplift, resulting in pile-up (section 3.2), occur simultaneously. This stress pattern ties in well with the lateral cracks, which are known to appear below the irreversibly deformed material area more or less at the end of unloading, depending on the exact type of glass [2].

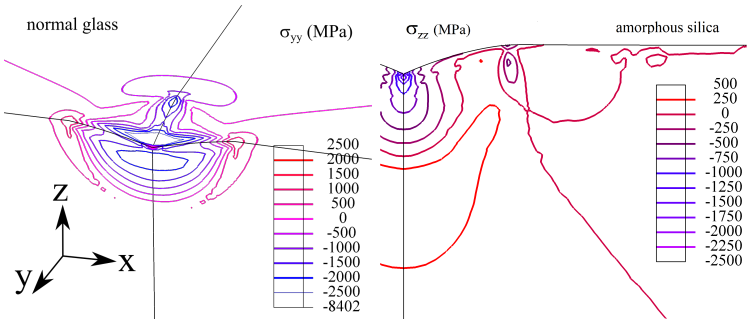

Figure 6: Vickers indentation, after full unloading. Left: distribution of stress component σ_{yy} in Vickers indentation after full unloading ($\tau_c = 3.5$ GPa, $p_c = 7.0$ GPa, $\Delta\rho_{sat} = 0.04$). The stress is maximum (tensile maximum $\sigma_{yy} = 1.345$ GPa) along the edges, which can give rise to the opening of radial cracks. Right: distribution of stress component σ_{zz} in Vickers indentation after full unloading ($\tau_c = 7.0$ GPa, $p_c = 9.0$ GPa, $\Delta\rho_{sat} = 0.20$). Tensile vertical stresses arise below the plastically deformed region right at the end of the unloading phase, consistent with the formation of lateral cracks.

As another example, the maximum principle stress calculated under load for a conical indenter equivalent to a Vickers is shown in Fig. 7 (top left) for an amorphous silica analog. The largest tensile value lies at the edge of the contact: it is predominantly a tensile stress parallel to the surface which, if cracking occurs, will produce ring cracks during loading. There is also another local stress maximum right below the plastically deformed area. This tensile stress component, which is normal to the axis of symmetry, can give rise to median cracking at high enough loads.

Since the stress distributions found in the numerical calculations match the well known crack patterns which are found to appear during glass indentation, we can now evaluate the relative impact of flow stress and densification on these stress fields.

Let us consider the reference silica analog and suppress densification by switching densification at saturation from 0.2 to 0.01, keeping all other parameters constant. The resulting maximum principal stress distribution is plotted in Fig. 7 (top right). Comparing to the densifying material (top left), we find that the overall stress distributions are very similar. In more detail, the overall stress level increases slightly when densification is switched out, and so does the spatial extent of the stress distribution. All in all, however, suppressing densification is found to affect stress fields only marginally. This conclusion parallels our previous comments on hardness.

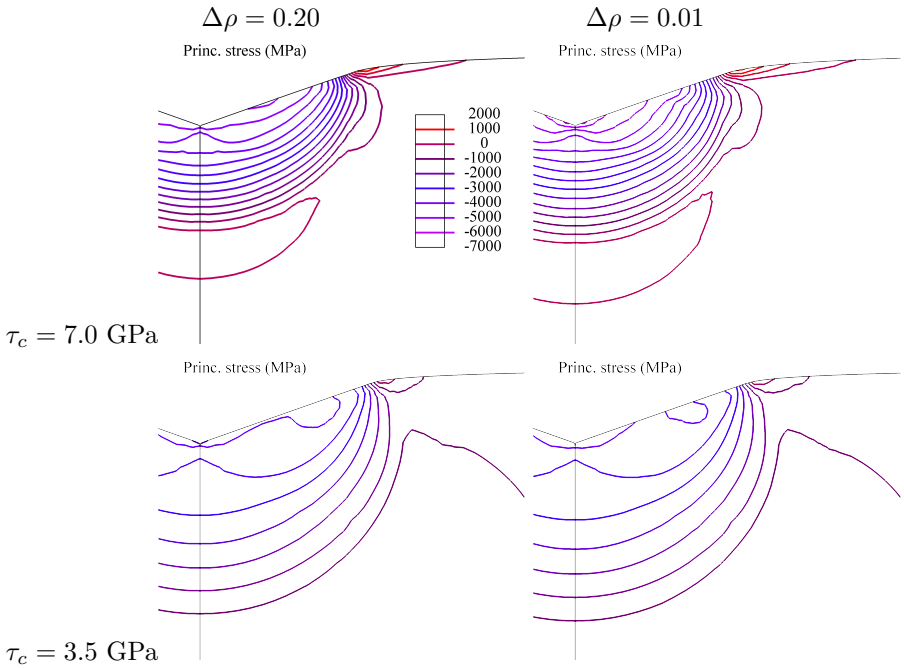

Figure 7: Maximum principal stress distribution for a Vickers equivalent cone indentation under load (p_c =9 GPa). Top: τ_c =7.0 GPa; bottom: τ_c =3.5 GPa; left: $\Delta\rho_{sat} = 0.20$; right: $\Delta\rho_{sat} = 0.01$.

Let us now consider the impact of flow stress. Lowering flow stress from 7.0 GPa to 3.5 GPa while keeping all the other parameters constant, we obtain the maximum principal stress patterns shown in Fig. 7 - bottom) for high (left - 0.20) or low (right - 0.01) densification at saturation. The general stress level under load is lower by ca 40% and the affected region is somewhat larger while the overall distribution is quite similar. This drop in stress level between (roughly speaking) amorphous silica and soda-lime glass is in fact proportional to the hardness reduction (Fig. 2), or equivalently to the flow stress reduction (see below). The densification at saturation is again seen to have an impact on stress distribution, but it is second order.

4. Discussion

4.1. Indentation of silicate glasses and confinement

When the indenter tip is pressed against the half-space, it imposes a set distribution of surface displacement so that under the resulting stress field, the substrate material under the tip is both elastically and plastically displaced into the half-space (Fig. 8).

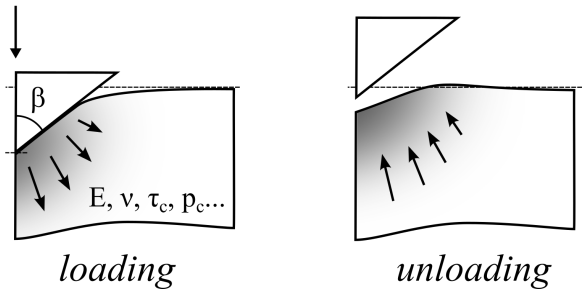

Figure 8: Schematics of pile-up formation upon unloading for silicate glasses.

Upon unloading, this irreversibly deformed core is pushed back by the elastically compressed half-space, giving rise to both pile-up (Fig. 5) and complex stress distributions (Fig. 6). It is these complex stress fields which are approximated by the combination of Boussinesq and blister fields in Yoffe's model [12].

Note also that for silicates, in the kinematics of pile-up formation, there is no material flow along the indenter faces upon loading. This latter phenomenology may be adequate for materials with much lower yield stresses over shear modulus ratios, such as metals with negligible hardening [22]. It is not consistent with silicate glass plasticity where the flow stress to shear modulus ratio is significantly larger than for typical metals. The difference between silicate glasses and other materials in this respect is demonstrated in Fig. 9 where we have plotted a number of literature values [23, 24] as a function of sample size. Amorphous silica definitely surpasses the other inorganic solids, even if the well-known size effect in crystalline materials [23] reduces the difference.

This phenomenology of indentation highlights the operation of confinement. The primary role of the flow stress to shear modulus ratio is to quantify the resistance to plastic strain effected by the surrounding elastic half-space.

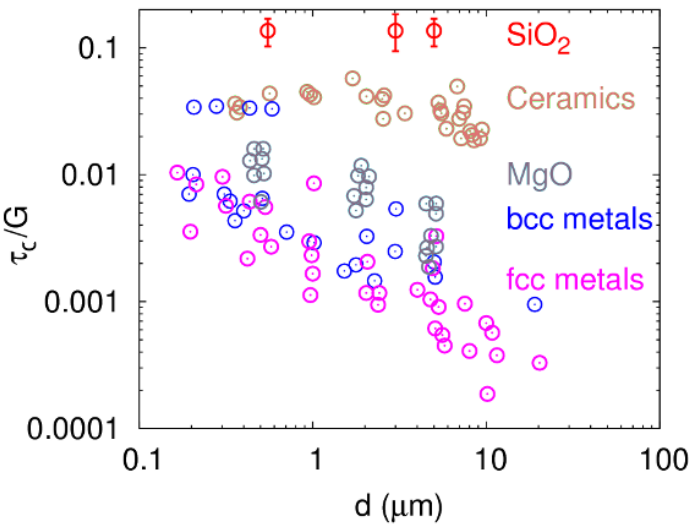

Figure 9: Flow stress normalized to shear modulus as a function of sample size in a broad range of materials (data from [23]) and in amorphous silica (data from [24]). Even at lower characteristic sizes, amorphous silica exhibits a larger τ_c/G ratio.

4.2. The constraint factor

Our numerical results suggest that densification is only a second order effect. We therefore expect that hardness in silicate glasses is dominated by the competition between plastic flow and elastic strain, as in standard, non-densifying materials. It is natural in this case to scale hardness by the flow stress: this ratio is the *constraint factor* [22, 25]. Note that sometimes this terminology is used only when the indentation regime is fully plastic, in which case the ratio is a constant [21, 26]. Here, because of the competition between plastic flow and elastic confinement, the constraint factor depends upon the ratio of flow stress to Young's modulus, as shown in Fig. 10 (left) for $\Delta\rho_{sat} = 0.01$. Due to self-similarity, the scaling of the numerical results is perfect within numerical error. At low τ_c/E, we recover the fully plastic regime where the constraint factor saturates to a finite value slightly lower than 3 as predicted by Tabor [22]. This saturation reflects the linear behaviour found in Fig. 2 left. At high τ_c/E values, the constraint factor decreases linearly, which explains the plateau at high τ_c in Fig. 2 left, especially for lower moduli. Unsurprisingly, given our observations on the moderate role of densification, the predictions of a phenomenological model proposed for isochoric plastic response (J2 plasticity) [27] are very close to the present values. In our case, the other material parameters also play a role, although less significant than flow stress, which is particularly relevant here since amorphous silica is perfectly plastic (*i.e.* the flow stress is independent of the plastic shear strain) [15]. For example, for a yield pressure $p_c = 9$ Gpa, the constraint factor is only moderately affected when densification at saturation $\Delta\rho_{sat}$ increases from 0.01 to 0.20 (Fig. 10 right). This result was expected from

the previous discussion. A slightly larger effect is registered for $\Delta\rho_{sat} = 0.2$ if the yield pressure decreases to $p_c = 5$ GPa. The master curve becomes really different if we assume that p_c varies proportionally to τ_c, at fixed densification at saturation $\Delta\rho_{sat}$.

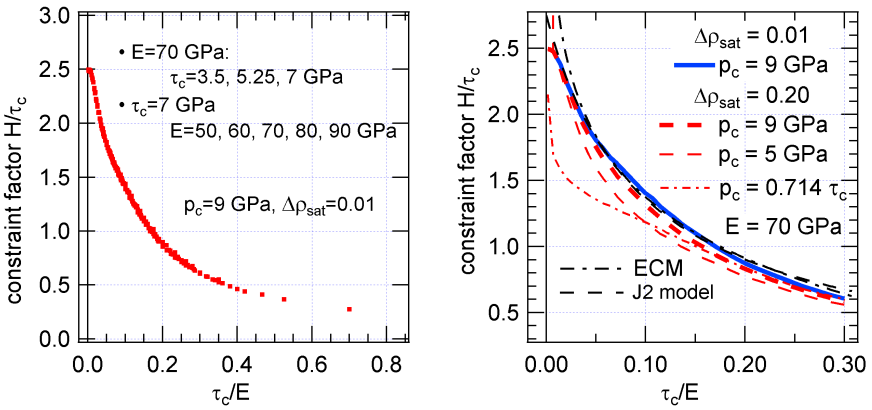

Figure 10: Rescaling hardness by flow stress (constraint factor) and flow stress by Young's modulus (cf. Fig. 4), a universal curve is obtained for a low value of densification at saturation 0.01 (left). The variations around this universal curve is very limited except if high densification at saturation comes along with low yield pressure (right, thin dashed and dot-dash red lines). A pure shear flow model (J2 plasticity, based on a simple von Mises criterion – dashed black line) effectively fits the numerical results, in the range relevant for most materials, including glasses ($\tau_c/E < 0.1$). The Expanding Cavity Model (dot-dash black line) also provides a good approximation in the relevant range of τ_c/E values but deviates for values below 0.05.

As already mentioned, one can use the phenomenological function for the constraint factor based on J2 plasticity [27] to predict the constrain factor with reasonable accuracy. For a slightly more refined prediction, we also propose two fits to our numerical results. For a negligible densification at saturation, a reasonable fit is given by

$$H/\tau_c = 0.42 + 2.12 \exp\left(-7.80\tau_c/E\right)$$

while for 0.20 densification at saturation and a 9 GPa yield pressure, an approximate relation is given by

$$H/\tau_c = 0.49 + 2.07 \exp\left(-9.26\tau_c/E\right)$$

With these expressions, flow stress can be easily determined directly from hardness, provided Young's modulus is known and a Vickers (or the nearly equivalent Berkovich) tip is used. This evaluation of the flow stress could be refined if other parameters such as Poisson's ratio and the densification parameters (yield pressure and pressure hardening parameters, including densification at saturation) are known. If other tips with different half included angles β are used, the J2

plasticity phenomenological model [27] can be used instead. It predicts

$$\frac{H}{\tau_c} = \frac{\zeta_1 \tan\beta}{(1-\zeta_2)\frac{\tau_c}{E} + \zeta_3 \tan\beta}$$

where the ζ constants are weakly dependent upon β.

Our numerical results can also be compared to the Expanding Cavity Model (ECM) introduced by Marsh [28] in the specific context of silicate glasses and propounded by Johnson a few years later [29]:

$$\frac{H}{\tau_c} = \frac{2}{3}\left[1 + \ln\left(\frac{1}{3}\frac{E}{\tau_c}\tan\beta\right)\right] + \frac{2}{3}$$

Note the additional 2/3 term as prescribed in [30]. It is seen (Fig. 10) that in the range of comparatively large τ_c/E ratios relevant for silicate glasses, the ECM model provides an equally good approximation as the J2 model. It is only at low τ_c/E ratios (and larger constraint factors - Fig. 10) that the validity of the ECM model becomes questionable.

In fact, in the ECM model, it is postulated that the subsurface displacements are radial [28, 29] (Fig. 8). This kinematic assumption is completely in line with the quasi absence of pile-up as indicated in sec. 3.2 and 4.1, in contrast to the slip line theory for rigid perfectly plastic materials, which is found adequate for low τ_c/E materials.

4.3. But what about indentation cracking?

We have found that the stress fields calculated numerically with the present constitutive relation are consistent with the phenomenology of indentation cracking [2, 4, 12].

However, we find little difference between the stress fields calculated with and without densification (Fig. 7). Just as with hardness (Fig. 2 and 3), densification would impact stress distribution for high enough densification at saturation and low enough effective yield pressure. However, due to the moderate value of the flow stress and the presence of hardening in the volumetric plastic deformation process, we find that densification impacts stress fields only marginally, even for a saturation value as large as 0.20. The practical consequences of this fact can be observed in a recent publication: when computing crack extension in amorphous silica, Bruns *et al.* found a minute effect of densification for a Vickers indenter and had to use sharper geometries to cranck up the impact [3].

Here again, it is shear flow, not densification, which primarily controls the stress distribution (Fig. 7), just as for hardness. The main differences between the stress fields of amorphous silica and normal glasses are due to: 1) the larger hardness (hence flow stress) of amorphous silica (9 GPa *vs. ca.* 6 GPa - Fig. 2), resulting in an overall higher stress level 2) the larger τ_c/E ratio (a factor of 2) resulting in some variation in the stress distribution pattern (Fig. 7).

Here, we make the observation that efforts to improve our understanding of cracking in silicate glasses have always been frustrated by a nagging problem: the narrow range spanned by the seemingly pertinent mechanical parameters

(elastic, plastic and rupture toughness). For example, Sellappan *et al.* have investigated a wide range of glasses [4], and from their tables, it is clear that elastic modulus and hardness change little: there is at most a factor of 2 between extremes. The effect of Poisson's ratio as an elastic parameter is quite limited (Fig. 4). As to the yield pressure, there are very few data [31, 32, 19, 33], but the measured values range between 6 and 9 GPa, and the densities at saturation between 1 and 1.2 times the density of the pristine material. Fracture toughnesses are remarkably similar between all sorts of glasses... In the classical picture, densification at saturation is the one parameter which changes considerably between silicate glasses: up to a factor 5! However, our results demonstrate that little effect must be expected from densification, so that the problem emerges with renewed acuteness: why are silicate glasses so diverse in their cracking resistance [34, 35] when they are so much alike in all their other mechanical properties? why are the cracking patterns definitely different from one family of glasses to the other, for example between anomalous and normal glasses [2], and even within a glass family? how can we explain a factor of ten improvement in crack resistance with moderate changes of composition in borosilicates [5]? what are the mechanical parameters responsible for indentation cracking...?

4.4. Crack initiation in silicate glasses - beyond the stress field

To answer these questions, we have to consider another phenomenon which has been largely overlooked in the recent literature: crack initiation. The stress distribution is relevant to predict the *propagation* of a crack, but on its own it cannot predict whether a crack will *form at all*. It determines only where a crack would go, if it formed. Possible mechanisms for crack initiation must be considered as well.

In this respect, we note that in the field of silicate glasses, shear flow is often thought of as resulting from shear bands. However, in many cases, shear flow is a homogeneous process, as observed in a large number of systems from metallic materials (at a length scale larger than the grains) to many liquids (at low strain rates). If shear bands are not observed, it does not mean there is no shear flow. In fact, the contribution of shear flow in the plastic deformation of amorphous silica is significant. This is demonstrated by the kinematics of our pillar compression experiments [24, 15], where the material necessarily flows to the sides as the micropillars are irreversibly turned into pancakes. Indeed, in the pillar geometry, the confinement inherent to indentation has been suppressed, and shear flow is unrestricted. Clearly, this shear flow is homogeneous: no shear band has been observed in these quasi-static experiments.

In many silicate glasses, however, the formation of shear bands is indeed observed [36]. This is not an oddity: shear bands are common in many disordered materials such as glassy polymers [37], bulk metallic glasses [26, 38] or granular materials [39]. They form due to flow instability and result in a strongly heterogeneous strain field, with strongly localized shear flow in the bands. It is precisely this propensity of many silicate glasses to undergo shear flow localization, and potentially strong material damage inside these bands, which opens up for significant differentiation between glass compositions. This is all

the more pertinent as crack initiation will result from a complex combination of tensile stress *and* material damage, which depend upon loading (damage) and unloading (residual tension) during one indentation cycle.

As early as 1979, Hagan has proposed that crack initiation in normal glasses starts from the intersection of shear bands [40] as previously observed in a glassy polymer such as polysterene [37]. These papers draw our attention to plastic induced damage, which is typically incurred through shear flow, and especially through *inhomogeneous* shear flow, *i.e.* shear bands. Recently, Gross et al. have examined a series of aluminoborosilicates and concluded that the glasses more resistant to indentation cracking exhibit finer shear bands, *i.e.* a more homogeneous flow [41]. More homogeneous shear flow as in boron-rich glasses means less damage and higher crack resistance. Similarly, amorphous silica undergoes homogeneous shear flow [15] which limits plastic induced damage. This is likely the reason why silica is less susceptible to median/radial cracking and usually (but not always [42]) develop ring/cone cracks instead. Ring/cone crack formation is an extrinsic process originating on (usually ill-defined) surface defects, which will also be favored by the larger overall stress level due to the high flow stress of amorphous silica.

We believe that developing constitutive relations is a necessary step to make progress in our understanding of the cracking resistance of silicate glasses. With good constitutive relations, precise stress fields can be calculated. Shear flow is an integral part of the plastic response of all silicate glasses, be it homogeneous or not. More precise descriptions of shear flow must indeed be developed. In particular, taking into account plasticity, and especially shear localization as a source of *material damage* opens up a different perspective for our understanding of indentation cracking in silicate glasses. In this respect, the constitutive equation used here is too restrictive. In particular, we have assumed perfect plasticity, which means in particular that shear flow is not softening: this is adequate for amorphous silica, but not for more normal glasses. If this simplifying assumption is lifted, using more advanced models [16], shear flow localization and the resulting material damage can be evaluated as well. In combination with the calculation of the stress field, quantitative assessment of material damage will lead to a significantly improved understanding of the nucleation and propagation of cracks under indentation loading.

5. Conclusion

Our calculations strongly suggest that the impact of densification on indentation response in silicate glasses has been consistently overrated over the last half-century. Even with significant densification at saturation, the contribution of densification to indentation response is limited due to the relatively high value of yield pressure compared to flow stress. In addition, it is an effective yield pressure involving hardening for irreversible volumetric strain which must be considered, and compared to a flow stress free from any hardening, at best. We conclude that flow stress is the determining factor for indentation response. As Marsh already put it more than half a century ago: "Even for silica

[...] compaction effects are probably much less important than was previously thought" [28].

Moreover, at the present level of description, it is clear that there is a missing piece in the standard description: cracking is varied for silicate glasses which are otherwise not differentiated by their elastic or plastic properties. We argue that the missing piece is damage sensitivity. Shear flow instability, and especially shear band formation is certainly a most interesting - but difficult - field to investigate in relation to this question.

Acknowledgements - we thank Rémi Lacroix for compiling the data for Fig. 9, René Gy for sharing his longtime interest in these questions, as well as numerous and helpful suggestions, Brian Davis and Shef Baker for in depth discussions of many aspects of this problem, Gergely Molnar for kindly providing the UMAT and a referee for suggesting the very relevant addition of the ECM model.

References

[1] AJ Dalladay and F Twyman. The stress conditions surrounding a diamond cut in glass. *Transactions of the Optical Society*, 23(3):165, 1922.

[2] Robert F Cook and George M Pharr. Direct observation and analysis of indentation cracking in glasses and ceramics. *Journal of the American Ceramic Society*, 73(4):787–817, 1990.

[3] Sebastian Bruns, Kurt E Johanns, Hamad UR Rehman, George M Pharr, and Karsten Durst. Constitutive modeling of indentation cracking in fused silica. *Journal of the American Ceramic Society*, 100(5):1928–1940, 2017.

[4] P Sellappan, Tanguy Rouxel, F Celarie, E Becker, P Houizot, and R Conradt. Composition dependence of indentation deformation and indentation cracking in glass. *Acta Materialia*, 61(16):5949–5965, 2013.

[5] Marina Barlet, Jean-Marc Delaye, Thibault Charpentier, Mickael Gennisson, Daniel Bonamy, Tanguy Rouxel, and Cindy L Rountree. Hardness and toughness of sodium borosilicate glasses via vickers's indentations. *Journal of Non-Crystalline Solids*, 417:66–79, 2015.

[6] R Limbach, A Winterstein-Beckmann, J Dellith, D Möncke, and L Wondraczek. Plasticity, crack initiation and defect resistance in alkali-borosilicate glasses: from normal to anomalous behavior. *Journal of Non-Crystalline Solids*, 417:15–27, 2015.

[7] TM Gross. Deformation and cracking behavior of glasses indented with diamond tips of various sharpness. *Journal of Non-Crystalline Solids*, 358(24):3445–3452, 2012.

[8] BA Mound and GM Pharr. Nanoindentation of fused quartz at loads near the cracking threshold. *Experimental Mechanics*, 59(3):369–380, 2019.

[9] Kacper Januchta and Morten M Smedskjaer. Indentation deformation in oxide glasses: Quantification, structural changes, and relation to cracking. *Journal of Non-Crystalline Solids: X*, 1:100007, 2019.

[10] Satoshi Yoshida. Indentation deformation and cracking in oxide glass–toward understanding of crack nucleation. *Journal of Non-Crystalline Solids: X*, 1:100009, 2019.

[11] F. M. Ernsberger. Role of Densification in Deformation of Glasses Under Point Loading. *J. Am. Ceram. Soc.*, 51(10):545 – 547, 1968.

[12] EH Yoffe. Elastic stress fields caused by indenting brittle materials. *Philosophical Magazine A*, 46(4):617–628, 1982.

[13] Guillaume Kermouche, Etienne Barthel, D Vandembroucq, and Ph Dubujet. Mechanical modelling of indentation-induced densification in amorphous silica. *Acta Mater.*, 56(13):3222–3228, 2008.

[14] Vincent Keryvin, J-X Meng, Solène Gicquel, J-P Guin, Ludovic Charleux, J-C Sangleboeuf, Philippe Pilvin, Tanguy Rouxel, and Guenhaël Le Quilliec. Constitutive modeling of the densification process in silica glass under hydrostatic compression. *Acta Mater.*, 62:250–257, 2014.

[15] G Kermouche, G Guillonneau, J Michler, J Teisseire, and E Barthel. Perfectly plastic flow in silica glass. *Acta Mater.*, 114:146–153, 2016.

[16] Gergely Molnár, Guillaume Kermouche, and Etienne Barthel. Plastic response of amorphous silicates, from atomistic simulations to experiments–a general constitutive relation. *Mechanics of Materials*, 114:1–8, 2017.

[17] W.C. Oliver and G.M. Pharr. An improved technique for determining hardness and elastic modulus using load and displacement sensing indentation experiments. *Journal of Materials Research*, 7(6):1564–1583, 1992.

[18] H. Ji, V. Keryvin, T. Rouxel, and T. Hammouda. Densification of window glass under very high pressure and its relevance to Vickers indentation. *Scripta Mater.*, 55:1159 – 1162, 2006.

[19] T. Deschamps, C. Martinet, J. L. Bruneel, and B. Champagnon. Soda-lime silicate glass under hydrostatic pressure and indentation: a micro-Raman study. *Journal of Physics: Condensed Matter*, 23(3):035402, 2011.

[20] S. Yoshida, J.-C. Sangleboeuf, and T. Rouxel. Quantitative evaluation of indentation-induced densification in glass. *J. Mater. Res.*, 20(12):1 – 3, 2005.

[21] V Keryvin, L Charleux, R Hin, J-P Guin, and J-C Sangleboeuf. Mechanical behaviour of fully densified silica glass under vickers indentation. *Acta Materialia*, 129:492–499, 2017.

[22] David Tabor. The hardness of solids. *Review of physics in technology*, 1(3):145, 1970.

[23] S Korte and WJ Clegg. Discussion of the dependence of the effect of size on the yield stress in hard materials studied by microcompression of mgo. *Philosophical Magazine*, 91(7-9):1150–1162, 2011.

[24] R. Lacroix, G. Kermouche, J. Teisseire, and E. Barthel. Plastic deformation and residual stresses in amorphous silica pillars under uniaxial loading. *Acta Mater.*, 60(15):5555–5566, 2012.

[25] K Eswar Prasad, V Keryvin, and U Ramamurty. Pressure sensitive flow and constraint factor in amorphous materials below glass transition. *Journal of Materials Research*, 24(3):890–897, 2009.

[26] V Keryvin. Indentation of bulk metallic glasses: Relationships between shear bands observed around the prints and hardness. *Acta materialia*, 55(8):2565–2578, 2007.

[27] G Kermouche, JL Loubet, and JM Bergheau. Extraction of stress–strain curves of elastic–viscoplastic solids using conical/pyramidal indentation testing with application to polymers. *Mechanics of Materials*, 40(4-5):271–283, 2008.

[28] D. M. Marsh. Plastic Flow in Glass. *Proc. R. Soc. London, Ser. A*, 279(1378):420 – 435, 1964.

[29] KL Johnson. The correlation of indentation experiments. *Journal of the Mechanics and Physics of Solids*, 18(2):115–126, 1970.

[30] K.L. Johnson. *Contact Mechanics*. CUP, Cambridge, 1985.

[31] T. Rouxel, H. Ji, T. Hammouda, and A. Moreac. Poisson's Ratio and the Densification of Glass under High Pressure. *Phys. Rev. Lett.*, 100(61):225501, 2008.

[32] D. Vandembroucq, T. Deschamps, C. Coussa, A. Perriot, E. Barthel, B. Champagnon, and C. Martinet. Density hardening plasticity and mechanical aging of silica glass under pressure: A Raman spectroscopic study. *J. Phys.: Condens. Matter*, 20:485221, 2008.

[33] Yoshinari Kato, Hiroki Yamazaki, Satoshi Yoshida, Jun Matsuoka, and Masami Kanzaki. Measurements of density distribution around vickers indentation on commercial aluminoborosilicate and soda-lime silicate glasses by using micro raman spectroscopy. *Journal of Non-Crystalline Solids*, 358(24):3473–3480, 2012.

[34] Satoshi Yoshida, Atsuo Hidaka, and Jun Matsuoka. Crack initiation behavior of sodium aluminosilicate glasses. *Journal of non-crystalline solids*, 344(1):37–43, 2004.

[35] Yoshinari Kato, Hiroki Yamazaki, Satoshi Yoshida, and Jun Matsuoka. Effect of densification on crack initiation under vickers indentation test. *Journal of Non-Crystalline Solids*, 356(35-36):1768–1773, 2010.

[36] J. T. Hagan. Shear deformation under pyramidal indentations in soda-lime glass. *J. Mater. Sci.*, 15(6):1417 – 1424, 1980.

[37] JBC Wu and JCM Li. Slip processes in the deformation of polystyrene. *Journal of Materials Science*, 11(3):434–444, 1976.

[38] Frans Spaepen. A microscopic mechanism for steady state inhomogeneous flow in metallic glasses. *Acta Metall.*, 25(4):407–415, 1977.

[39] G Mandl, LNJ De Jong, and A Maltha. Shear zones in granular material. *Rock mechanics*, 9(2-3):95–144, 1977.

[40] JT Hagan. Micromechanics of crack nucleation during indentations. *Journal of Materials Science*, 14(12):2975–2980, 1979.

[41] TM Gross, J Wu, DE Baker, JJ Price, and R Yongsunthon. Crack-resistant glass with high shear band density. *Journal of Non-Crystalline Solids*, 494:13–20, 2018.

[42] A Arora, DB Marshall, BR Lawn, and MV Swain. Indentation deformation/fracture of normal and anomalous glasses. *J. Non-Cryst. Solids*, 31(3):415–428, 1979.